UNSTEADY LOADS EVALUATION FOR A WIND TURBINE ROTOR

Said CHKIR*, Ivan DOBREV**, Patrick KUSZLA***, Fawaz MASSOUH****

* Arts et métiers ParisTech, ERDT
151 Bd de l'Hôpital, 75013 Paris, France, said.chkir@paris.ensam.fr
** Arts et métiers ParisTech, LMF
151 Bd de l'Hôpital, 75013 Paris, France, ivan.dobrev@paris.ensam.fr
*** Arts et métiers ParisTech, DYNFLUID
151 Bd de l'Hôpital, 75013 Paris, France, patrick.kuszla@paris.ensam.fr
**** Arts et métiers ParisTech, ERDT, LMF
151 Bd de l'Hôpital, 75013 Paris, France, fawaz.massouh@paris.ensam.fr

Summary

This paper presents a method for calculating the flow around a wind turbine rotor. The real flow is replaced by a free stream past a vortex model of the rotor. This model consists of lifting vortex lines which replace the blades and a trailing free vorticity. The vorticity shed from the blade is concentrated in two vortices issued from tip and root. To compute the unsteady forces exerted on the rotor, a free wake method is used. The evolution of the wake is obtained by tracking the markers representing the vortices issued from the blade tips and roots. To solve the wake governing equation and to obtain the marker positions, a time-marching method is applied and the solution is obtained by a second order predictor-corrector scheme. To validate the proposed method a comparison is made with experimental data obtained in the case of a model of wind turbine where the flow field immediately behind the rotor is measured by means of PIV. It is shown that the numerical simulation captures correctly the near wake development. The comparison shows satisfactory accuracy for the velocity field downstream of the rotor.

Keywords: Wind turbine/Unsteady aerodynamics/Vortex/Wake/PIV.

NOMENCLATURE

α : Lamb-Oseen constant
δ : Effective eddy-viscosity coefficient
$\vec{r}$: Position vector of vortex control point
t_0 : Initial position at time t = 0
ψ_w : Vortex wake age (rad)
ψ_b : Azimuthal angle (rad)
V_∞ : Free-stream velocity vector
Γ : Vortex strength, Circulation (m/s)
ρ : Density of air
N : Number of rotor blades
c : Blade chord
W : Wind relative velocity
V_{ind} : Induced velocity vector
r_t : Blade tip radius, (m)
r_h : Blade root radius, (m)
ds : Element of the vortex.
r_0 : Initial viscous core radius
r_c : Viscous core radius
a_1 : Turbulent viscosity constant
Re_v : Vortex Reynolds number
Ω: Rotational speed of the rotor (rad/s)
ϕ : Flow angle
v_i : Self-induced velocity at point i
Δs: Vortex segment length
C_L : Lift coefficient
C_D : Drag coefficient

INTRODUCTION

In the last few decades, wind energy has become the leading contender among the renewable sources of energy. Wind turbines are playing a significantly increasing role in the generation of electrical power that can then be used in various applications. Wind turbines operate in a complex unsteady flow environment composed of various effects such as atmospheric turbulence, ground boundary layer effects, directional and spatial variations in wind shear and the effects of the tower shadow. The estimation of the velocity field and local angle of attack of the blade's profiles could be the key to predict the aerodynamic loads on the rotor and the power generated by a wind turbine.

Improving the capability of the numerical tools to predict the aerodynamic and mechanical forces applied to the rotor, is one of the most important factors to optimize their design, operating and maintenance costs and to verify their reliability.

Generally, methods concerned with the prediction of the aerodynamic loading and performance of wind turbines assume that the fluid is inviscid and incompressible. In the most common method, the Blade Element Momentum Theory (BEM) methods [1], the blade is divided into several segments with cylindrical surfaces and the calculation is performed segment by segment. All blade elements are assumed to operate independently of each other. Accordingly, if lift and drag forces are determined for each element; it will be then possible to evaluate the rotor characteristics. In the present free wake method, the airfoil relative velocity is corrected by the induced velocity. The axial and tangential induced velocities are calculated for each section using the momentum theorem. The BEM methods are simple to use, require little computer time and provide accurate results, however, it contains invalid assumptions which are overcome in practice by empirical adjustments.

In recent years the resolution of the Navier-Stokes equations [2] has become a preferred method in all the domains of fluid mechanics. The advantages of this method are well known, especially the possibility of obtaining a solution in very complex flows cases. Despite the good results in most cases, these methods need huge computational costs and large memory requirements that delayed their practical use for many problems, including helicopter and wind turbine applications.

The vortex methods are potential methods based on the replacement of the real flow through the rotor by an inviscid fluid flow through an equivalent vortex system. This system consists of blade attached vortices and free vortices trailed into the wake. According to the representation manner of the vortex wake, there are two different approaches: prescribed wake and free wake. The prescribed wake method assumes that the wake shape is known, either through testing, or from an approached calculation [3]. In unsteady conditions and if the induced velocity is important, the wake shape varies in time and the prescribed wake method is therefore not applicable. In this case, the free wake method is preferred and we will describe its principles in the following.

1. METHODOLOGY

The free wake method is originally used in the analysis of helicopter rotors [4]. These models created for helicopter rotors have been later adapted for the calculation of wind turbines rotors [5]. In this vortex method, the real flow is replaced by an inviscid fluid flow through an equivalent vortex system.

This system consists of vortex attached to each blade (exerting on the fluid the same forces as those applied by the blades) and a wake consisting of a strong tip-vortex emanating from each blade tip and root (Fig. 1).

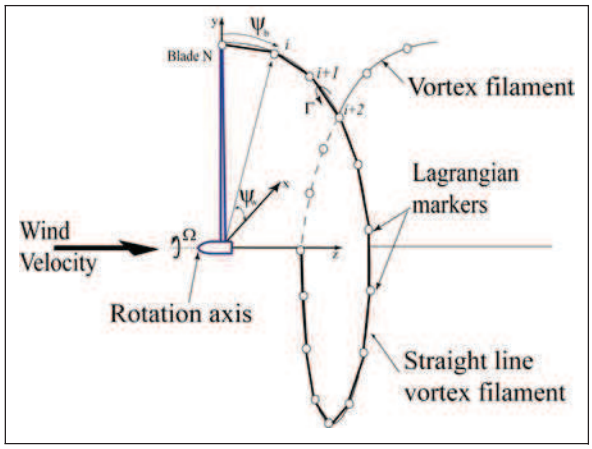

Fig. 1. Representation of the rotor wake

In this work, a Lagrangian description of the flow is used. Lagrangian markers are distributed along each tip-vortex filament (Fig. 2). Thus, tip-vortex filaments are discretized and the markers are linked together, usually with straight line segments. This allows the induced velocity to be determinated using the Biot-Savart law:

$$d\vec{V}_{ind} = \frac{\Gamma}{4\pi}\frac{d\vec{s}\times\vec{r}}{|\vec{r}|^3}. \qquad (1)$$

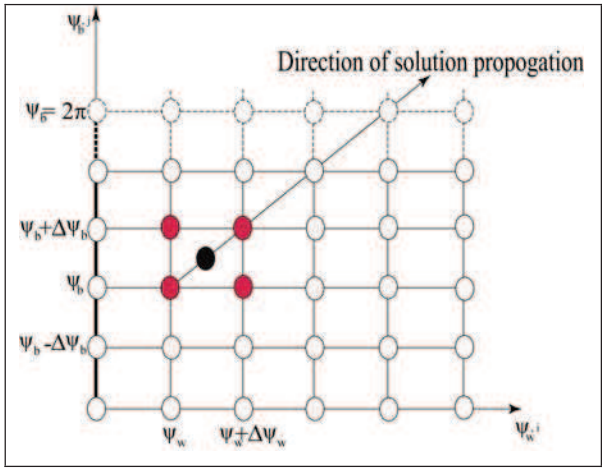

Fig. 2. Five-point central differencing scheme

The spatio-temporal evolution of the markers in the rotor wake can be derived from Helmholtz's law (vorticity transport theorem) by assuming that for each point in the flow the local vorticity is convected by the local velocity. The fundamental equation describing the transport of the filament is:

$$\frac{d\vec{r}}{dt} = \vec{V}. \qquad (2)$$

Where $\vec{r}$ is the position vector that can be represented using a function of two variables, which represent the spatio-temporal evolution of the Lagrangian markers position:

$$\vec{r} = \vec{r}(\psi_w, \psi_b) . \quad (3)$$

In equation (3), ψ_w is the azimuth angle (wake age) corresponding to the vortex that was trailed from the blade when it was at an azimuth angle ψ_b. Using these two angular variables and a constant angular velocity Ω of the wind turbine, the position vector $\vec{r}$ of a wake element can be expressed as a function of the azimuthal blade position ψ_b and the age of the filament ψ_w relative to the blade when it was introduced into the wake. Equation (2) can, therefore, be written in the non-rotating, hub-fixed coordinate system as:

$$\frac{\partial \vec{r}}{\partial \psi_w} + \frac{\partial \vec{r}}{\partial \psi_b} = \frac{1}{\Omega}\vec{V} . \quad (4)$$

where the velocity $\vec{V}$ is the contribution of the free stream and the highly nonlinear self and mutually induced velocities corresponding to the vortex wake structure. Note that equation (4) is a first-order, partial differential equation. The homogeneous portion of this equation is hyperbolic. However, the right-hand side, which includes the velocity induced by the attached and the free vortex, is highly nonlinear.

The complexity of the solution of equation (4) arises from the nonlinearity and the singularity of the vortex filaments. To simplify the calculation, the blade surface must be replaced by a vortex line with a constant circulation. This simplification can be justified in the case of high aspect ratio blades, as observed in wind turbines. A numerical solution of equation (4) may be made by using a second order predictor-corrector scheme to improve the accuracy and the stability of the numerical algorithm. The discretization of equation (4) is presented in (Fig. 2) using a five-point central differencing scheme.

The predictor step is used to obtain an intermediate solution at the new time step to enable the induced velocity calculation $\vec{V}^{\,n}_{j+\frac{1}{2}}$ to proceed by using Biot-Savart law as:

$$\tilde{\vec{r}}_{j+1} = \vec{r}^{\,n}_j + \frac{2}{\Omega}\left(\frac{\Delta\psi_w . \Delta\psi_b}{\Delta\psi_w + \Delta\psi_b}\right)\vec{V}^{\,n}_{j+\frac{1}{2}} \quad (5)$$

The corrector step is obtained by averaging the predicted induced velocity $\tilde{\vec{V}}_{j+\frac{1}{2}}$ with $\vec{V}_{j+\frac{1}{2}}$ at $(n)^{th}$ time step as:

$$\vec{V}^{\,n+\frac{1}{2}}_{j+\frac{1}{2}} = \frac{1}{2}\left(\vec{V}^{\,n}_{j+\frac{1}{2}} + \tilde{\vec{V}}_{j+\frac{1}{2}}\right). \quad (6)$$

Then, this value is used with the obtained value of (5) in the corrector step as:

$$\tilde{\vec{r}}^{\,n+1}_{j+1} = \vec{r}^{\,n}_j + \frac{2}{\Omega}\left(\frac{\Delta\psi_w \Delta\psi_b}{\Delta\psi_w + \Delta\psi_b}\right)\vec{V}^{\,n+\frac{1}{2}}_{j+\frac{1}{2}} . \quad (7)$$

The local air velocity relative to the rotor blade consists of the free-stream velocity and the wake induced velocities as:

$$\vec{V} = \vec{V}_\infty + \vec{V}_{ind} . \quad (8)$$

The wake induced velocity is evaluated by the application of the Biot-Savart law (1) as an integral along the complete length of each vortex wake filament. For a vortex segment of length AB (Fig. 3), the induced velocity at a point C can be written as:

$$d\vec{V}_{ind\,C} = \frac{\Gamma}{4\pi}(\vec{r}_1 \times \vec{r}_2)\frac{1}{|\vec{r}_1|\cdot|\vec{r}_2| + \vec{r}_1 \cdot \vec{r}_2}\frac{|\vec{r}_1| + |\vec{r}_2|}{|\vec{r}_1|\cdot|\vec{r}_2|} . \quad (9)$$

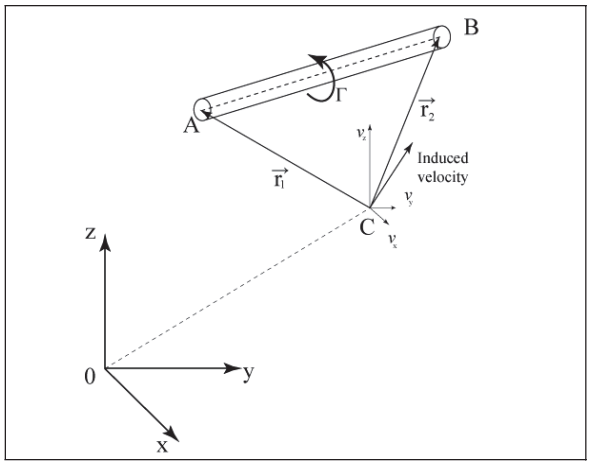

Fig. 3. Induced velocity by a segment vortex

At the control point, where we have to calculate the self induced velocity, equation (9) is singular. However, a straight vortex representation cannot induce a velocity on itself, the contribution of vortex straight-segment at the left and right of the control point is zero, so a curvature correction should be applied [6]. The correction is applied only at the neighboring of the control point, where the self-induced velocity is needed. The theoretical velocity on the vortex line is infinite. But in the real case, a vortex tube is observed. The maximum velocity induced by this tube can be found on the surface of the vortex core of radius r_c. The self-induced velocity can be calculated by an integration of the Biot-Savart law along a curved vortex filament excluding the vortex core (Fig.4).

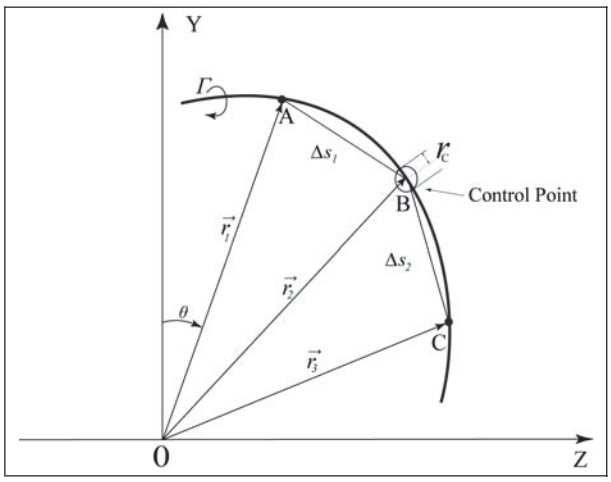

Fig. 4. Calculation of the self-induced velocity

This treatment gives the formula proposed by Hama [7]

$$\vec{v}_i = -\frac{\Gamma(\frac{\partial \vec{r}}{\partial s}) \times (\frac{\partial^2 \vec{r}}{\partial s^2})}{4\pi \left|\frac{\partial \vec{r}}{\partial s}\right|^3} \ln r_c \,. \qquad (10)$$

In our case, the value of r_c is in order of 10 % of the tip airfoil chord. It represents the core radius of the viscous vortex and allows taking into account his actual structure. The radius r_c can be obtained either from experiments or from semi-empirical laws.

Because of the viscous effects, the core radius of the tip vortices does not remain constant and increases as it progresses downstream of the rotor. Leishman and Bhagwat [8] suggested an empirical approach to calculate the growth of the viscous core radius:

$$r_c(\psi_w) = \sqrt{r_0^2 + \frac{4\alpha\delta\nu\psi_w}{\Omega}} \,. \qquad (11)$$

Here, the eddy-viscosity coefficients δ takes into account the diffusion rate of the tip vortex, which must be a function of the Reynolds number as:

$$\delta = 1 + a_1 \mathrm{Re}_v \,. \qquad (12)$$

The experimental values of α and a_1 are given in [9]. It is observed also that the circulation Γ decreases along the vortex filament, this is caused by viscous dissipation. Indeed, this circulation reduction is taken into account from experimental data.

1.1. Numerical algorithm

The calculation is initialized with all the vortex markers located at the tip vortex of the blades. At each time step one vortex segment is emitted and moves with the local fluid velocity. The modified vortex structure changes the induced velocity field. The updated velocities are then used to move the markers using the described predictor-corrector scheme. For the presented calculation, each vortex filament was discretized by 200 segments. A stable periodic configuration was obtained after 30 revolutions of the rotor.

At each time step, we also calculate the induced velocity along the blades axis. These induced velocities allow us to obtain the relative velocity distribution and the angles of attack along the blade. And finally the updated circulation is obtained using the Kutta-Joukowski lift theorem.

For the steady case, we can calculate the aerodynamic efforts exerted on a wind turbine rotor (the calculations of blade forces *F*, rotor torque *Q*, and the power *P)* by using the formula:

$$F = \int_{r_r}^{r_t} \frac{1}{2} \rho N c W^2 (C_L \cos\phi + C_D \sin\phi) dr \qquad (13)$$

$$Q = \int_{r_r}^{r_t} \frac{1}{2} \rho N c W^2 (C_L \sin\phi - C_D \cos\phi) r dr \qquad (14)$$

$$P = \int_{r_r}^{r_t} \frac{1}{2} \rho N c W^2 (C_L \sin\phi - C_D \cos\phi) r\Omega dr \qquad (15)$$

If the blades circulation does not vary any more, we stop the calculation, and then the aerodynamic characteristics of the wind turbine can be evaluated by (13), (14) and (15).

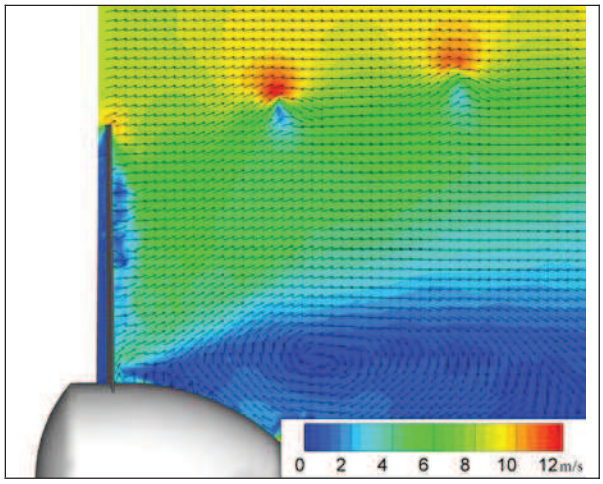

Fig 5. Downstream axial velocity field, Rutland 503 wind turbine (m/s), PIV measurement

2. RESULTS AND DISCUSSION

The calculation results show the robustness of the predictor-corrector scheme proposed. In order to validate this method, we present here only the wake calculation results witch compared with laboratory measurements made with PIV. The study focused on areas where wake modeling requires attention; in particular, to obtained the form trailing tip vortex, vital for the prediction of fluid loading on the rotor blades.

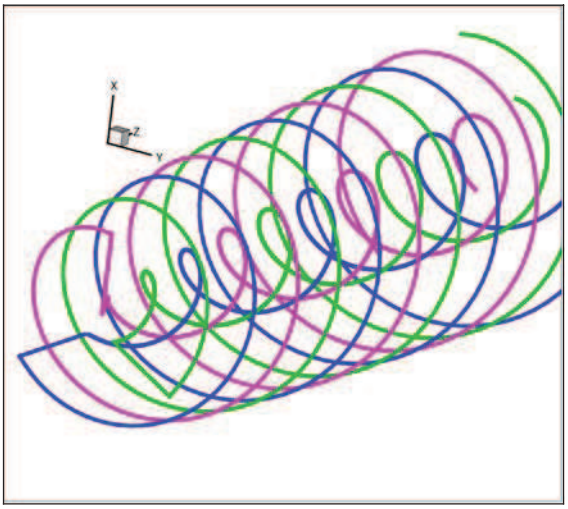

Fig. 6. Downstream wake shape calculated by the present free wake method, Rutland 503 wind turbine

The experimental data used for validation were obtained at the ENSAM-Paris wind tunnel using a modified commercial wind turbine Rutland 503, [10]. The PIV technique is applied to obtain the velocity in the wake downstream of the turbine rotor and also the vortex tip positions.

The horizontal axis wind turbine has a three blades rotor with a diameter of 0.5 m and a hub diameter of 0.135 m. The blades are tapered and untwisted. They have a pitch angle of 10° and a chord of 0.045 m at tip and 0,065 m at root. The rotational speed is 1000 rpm with a free-stream velocity of 9.3 m/s. The wind turbine is mounted on a support tube ensuring a sufficient height in order to allow the lasers fixed above the transparent roof to illuminate the explored plane with an adequate intensity.

The airfoil characteristics are important to calculate the circulation along the blade. Unfortunately the experimental data concerning Rutland airfoil sections is not available. It is possible to carried out CFD calculation and obtain the needed data, but to reduce the influence of blade airfoil characteristics on the calculation, the tip vortex intensity is prescribed. This circulation is the same as in experiments.

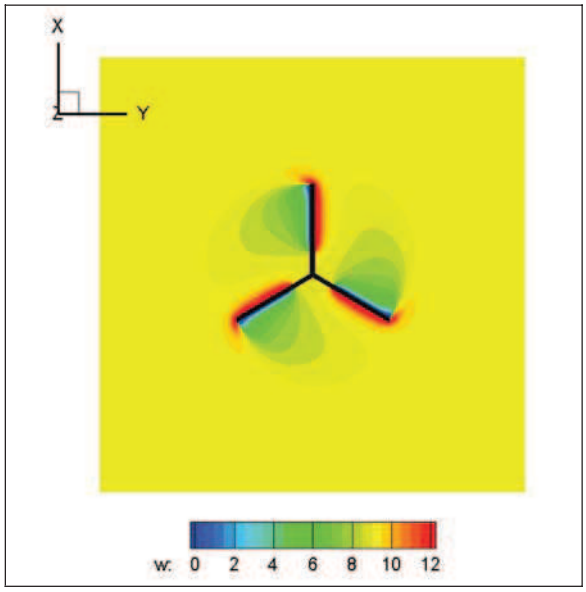

Fig. 7. Face view of the wake calculated by the present free-wake method, axial velocity (m/s)

The wake vortex shape is presented in (Fig.6), it generally fits the experimental wake shown in (Fig. 5). The axial velocity field in the rotor plane and in the azimuth plane is presented in (Fig.7). It may be noted, outside the wake, the wind is accelerated by the axial component of the induced velocity of all the vortices. However, in the wake, the induced velocity by the vortex is decelerating the flow. Accordingly, downstream of the turbine the wake diameter increases as the distance from the rotor increases. After some distance, the diameter remains constant in the simulation as in the experiment.

In the experiment (Fig. 5), we can see that there is a vortex area behind the hub which is not taken into account in our simulation. In fact, in the case of industrial turbines, the hub is much smaller and this stall area and recirculation does not exist.

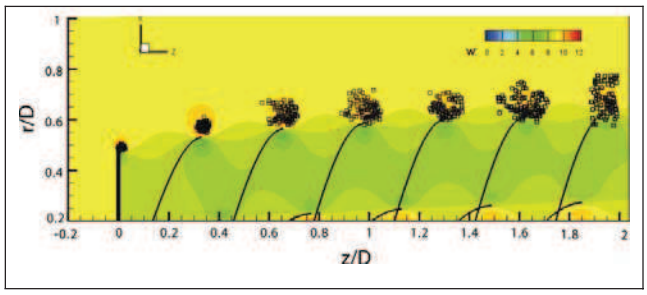

Fig. 8. Comparison of the tip vortex locations obtained from the free wake method and the PIV results

Figure (8) shows a comparison between the tip vortex positions obtained from the PIV experiment and the free wake method for axial (unyawed) flow conditions. The wake expands behind the turbine, and the free wake method captures the tip vortex locations well for younger wake ages. Some differences can be seen in the far wake. The increased uncertainly in defining the tip vortex

positions is partially due to the diffusion of the real vortex cores. In addition, some aperiodicity of the flow may account for the differences in the locations for older wake ages.

3. SUMMARY

This paper has reviewed the theoretical basis and numerical implementation of one class of a free wake method, which was set up to calculate the aerodynamic loadings and performance of a horizontal-axis wind turbine.

In this method, the rotor wake is discretized into vortex filaments defined by a series of Lagrangian markers. The governing equation for this free-wake problem is reduced to a system of first-order, partial differential equations that describe the convection of these markers through the flow.

Unlike the prescribed wake method, we calculate here explicitly the trajectory of vortex markers emitted by blade tips. The calculation results show that the wake has a helical-like form. Furthermore the vortex lines are not located on a cylindrical surface, as suggested by the linear vortex theory. They move outward by increasing the diameter of the vortex tube. A validation study for the prediction of the wake geometry behind a three-bladed wind turbine using a free-wake was performed for axial flow conditions, and was validated against laboratory experiments using the PIV technique. The comparison reveals that accurate results can be obtained, for the operating conditions considered, with substantial savings of computer time, comparing to the CFD method

REFERENCES

[1] Sørensen, JN., Mikkelsen, R.: *On the validity of the blade element momentum method*, Proceedings of the EWEC, Kopenhagen, 2001.
[2] Sørensen, J N., Michelsen, J., and Schreck, S. *Navier-Stokes predictions of the NREL phase VI rotor in the NASA Ames 80x120 ft wind tunnel.* Wind Energy, pp 151-169, 2002.
[3] Leishman, G. *Challenges in modeling the unsteady aerodynamics of wind turbines*, Wind Energy, 5(2-3):85-132, 2002.
[4] Leishman, G., *Principles of helicopter aerodynamics*. Cambridge Aero. Series., 2000.
[5] Afjeh, A, Keith T.: *A Simplified Free Wake Method for Horizontal-Axis Wind Turbine Performance Prediction*, Journal of fluid engineering vol. 108 pp 400-406. 1986.
[6] Wood, D. H.: *Generic vortex modeling for horizontal-axis wind turbine*, Wind Engineering, 26(2), pp. 71-84, 2002.
[7] Hama, F.: *Progressive Deformation of a Curved Vortex by Its Own Induction*, Physics of fluids, pp 1156-1162. 1962.
[8] Leishman, G., Bhagwat, M.: *Correlation of Helicopter Tip Vortex Measurement*, AIAA Journal, Vol. 38, No 2, pp.301-308, 2000.
[9] Ramasamy, M., Leishman, G., *Interdependence of Diffusion and Straining of Helicopter Blade Tip Vortices*, Journal of Aircraft, 41(5):1014-1024, 2004/
[10] Dobrev, I., Maallouf, B., Troldborg N., Massouh, F.: *Investigation of the Wind Turbine Vortex Structure*, 14th Int Symp on App. of Laser Tech. to Fluid Mech., Lisbon, 2008.

Said CHKIR
Researcher, Arts et Métiers ParisTech
France

Research interests: Fluid Mechanics, Wind energy

Ivan DOBREV
Researcher, Arts et Métiers ParisTech
France

Research interests: Fluid Mechanics, Wind energy.

Patrick KUSZLA
Qualified Professor, Arts et Métiers ParisTech, France

Research interests: Aerodynamics, Numerical simulation, Wind turbines, Simulation of manufacturing processes, Unmanned aerial vehicles

Fawaz MASSOUH
Assoc. Professor, Arts et Métiers ParisTech, France

Research interests: Fluid Mechanics, Wind energy.